# Analysis of Atmospheric Convection in the UAE with a Scanning Doppler Cloud Radar

**Nurudeen Adesina**

Institute of Physics and Meteorology, University of Hohenheim, Germany

**Abstract:** ***The Optimization of Cloud Seeding by Advanced Remote Sensing and Land Cover Modification (OCAL) experiment aims to detect convergence zones and convection initiation in the UAE. Convergence zones are possible zones of convection initiation. However, convection initiation is expressed by a variety of processes interacting on different spatial and time scale which may finally lead to deep convection. The investigation of such case over mountaneous terrain is presented in this paper. Data from the Doppler cloud radar are analyzed to determine convergence zones and convection initiation. EUMESAT 8, rain guage precipitation, weather radar and radiosonde data are also used to support the Doppler cloud radar data. The Doppler wind velocity and the Radar reflectivity inside the cloud are evaluated. A cummulonimbus cloud due to deep convection and causing convective precipitation is observed. Convergence lines and zones before precipitation are clearly observed some of which lead to ascent giving rise to cloud formation. During the summer, no precipitation reached the ground because of very low moisture content of the advecting air. During the winter, precipitation took place in some days.***

**Keywords:** Convection initiation, Convergence zones, deep convection, convective precipitation, cummulonimbus cloud

## 1. Introduction

The major challenge behind this study is to ensure water security in the arid region, especially in the UAE by detecting the precipitation formation processes. This is achieved by using improved observations from a scanning Doppler cloud radar by the advanced detection of convergence zones and convection initiation. This is based on the fact that new observations are required to improve process understanding, since models are only as good as the data used for their verification [2]. The investigation of convection initiation is governed by large-scale mainly upper tropospheric processes including regional and local-scale boundary-layer and orographically-driven processes.

Convection initiation (CI) is the beginning of atmospheric convection which may result in deep convection with severe weather like gust fronts, flash floods and thunderstorms. Therefore the conditions leading to CI are of great importance. It is necessary to include CI in nowcasting schemes as well as to represent CI in operational weather forecasting models. CI describes the processes which trigger coherent vertical motion of such strength that finally the level of free convection (LFC) is reached.

The interaction of convection-generating processes like orographic wind systems, moisture flux convergence, thermally direct circulations and mesoscale flow patterns is the prerequisite for CI [2]. Due to the interaction of these processes on different scales, locally and temporally very high gradients of meteorological parameters (humidity, temperature, pressure, wind) develop in the lower troposphere, which are acting as a jump start for convection [28].

## 2. Literature Survey

The UAEREP was initiated in the late 1990s against water crisis. A collaborative rain enhancement program between the Department of Water Resources Studies (DWRS) in the UAE, the University of the Witwatersrand in RSA, the South African Weather Service in RSA and the National Center for Atmospheric Research (NCAR) in USA was implemented in late 2000. Previously, satellite has been used in analyzing convergence zones and convection initiations. However, due to lower spatial and temporal resolution, and higher scanning times of satellite, radar has been recently and mostly used for the investigation of convective storm in the Eastern Arabian Peninsula. The use of Doppler cloud radar is beneficial because of its high spatial and temporal resolution, lower scanning times and relativelyscans large volumes of the atmosphere. Therefore, it provides high resolution measurements of reflectivity and radial velocity in forecasting quickly developing mesoscale systems.

## 3. Methodology

### 3.1 Case Study

In this study for the analysis of atmospheric convection involving the advanced detection of convergence zone and convection initiation in the UAE, the major data source is the radar. However three other data sources namely, METEOSAT 8, weather radar data and radiosonde meteorological data are used additionally to verify the radar data. The use of radar in studying these sites is advantageous due to its shorter scanning interval, higher resolution and quality, and smaller image distortion compared to satellite image with shorter scanning interval, lower resolution and quality and larger image distortion.

Basically, the method makes use of two data products from a scanning Doppler cloud radar, namely the radar reflectivity (RR) and Doppler wind velocity (DWV). From these measurements, the hydrometeor composition of clouds and wind fields can be determined. It is based on the fact that the Doppler cloud radar signals - unlike Doppler lidar signals, have low extinction in clouds. Thus, both top and bottom of clouds as well as their internal structure can be better observed. The Doppler cloud radar emits in the Ka band with frequency and wavelength of 37.5GHz and 8 mm respectively.

### 3.2 Radar scanning modes

The two major scan types used are the Plan Position Indicator (VAD) and the Range Height Indicator (RHI) scans. RHI scans imply that the radar holds the azimuth angle constant but varies the elevation angle. VAD means the radar holds the elevation angle constant but varies the azimuth angle. VAD surveillance scan ($360^0$) is used here. The radar is programmed to make RHI scans at azimuth angles 0, 30, 60, 90, 120 and 150 degrees. VAD scans are made at elevation angles 5 and 45 degrees in the UAE. RHI and VAD scanning modes were employed at regular time intervals. The elevation scan of the RHI ranges from $0^0$ to $180^0$. RHI scans take 2:02 minutes while VAD scans take 4:00 minutes (table 1).

## 4. Results

In the UAE, the data collection started on 12.09.2017 and continues up to the moment. The generated NetCDF files by the radar are converted to BSC files (Doppler wind velocity BSC files and radar reflectivity BSC files) and plotted with Interactive Data Language (IDL). For the illustration of case studies which may provide insights for the detection of convergence zones and convection initiation, data on 19.09.2017 were used during summer while data on 16.11.2017 and 18.12.2017 were used during winter. The examples of the plots, results and discussions of the data for each day are shown below.

**Table 1:** Radar scanning modes and velocity for both RHI and VAD scans

| RHI (elevation changes) | | VDA (azimuth changes) | |
|---|---|---|---|
| Azimuth angles (degrees) | Time (minutes) | Elevation angles (degrees) | Time (minutes) |
| 0 | 2:02 | 5 | 4:00 |
| 30 | 2:02 | 45 | 4:00 |
| 60 | 2:02 | | |
| 90 | 2:02 | | |
| 120 | 2:02 | | |
| 150 | 2:02 | | |

**Table 2:** Definitions of the ranges of values for the DWV and RR

| DWV | | | RR | |
|---|---|---|---|---|
| Direction | Defination | Range of values, m/s | Defination | Range of values, dB |
| Away | Low | 0 to -5 | very low | < -30 |
| Away | Medium | -5 to -10 | low | -30 to -10 |
| Away | High | < -10 | Medium | -10 to 10 |
| Towards | Low | 0 to 5 | High | 10 to 30 |
| Towards | Medium | 5 to 10 | very high | > 30 |
| Towards | High | > 10 | | |

### 4.1 Summer period on 19.09.2017

Cloud formation starts on 19.09.2017 at 12:09 UTC even though very few. The radial wind speed is low (<5m/s) and radial winddirection is west. By 12:12 UTC, the cloud becomes larger (figure 1a), with higher radial wind speed of about 10m/s (medium). A cumulonimbus cloud due to local convection is formed. The DWV field changes from SE at lower height to NW above as shown (figure 1a & b). The high reflectivity shows the presence of rain (figure 1a & b). However, much moisture is not present in the air to form more clouds that can sustain and cause precipitation at the Earth's surface. Shortly, the cloud disappears.

Consistently, the precipitation data also shows no precipitation. Although, some of the lifting mechanisms are present, the absence of moisture in the advecting air could not stabilize the thunderstorm. Since this is the largest cloud observed during measurement period over this area, very low precipitation occurs during the summer. Correspondingly, the EUMESAT 8 image of the UAE study site confirms cloud presence over the Al - Farfar mountain.

**Left azimuth=$300^0$** **Right azimuth=$480^0$**

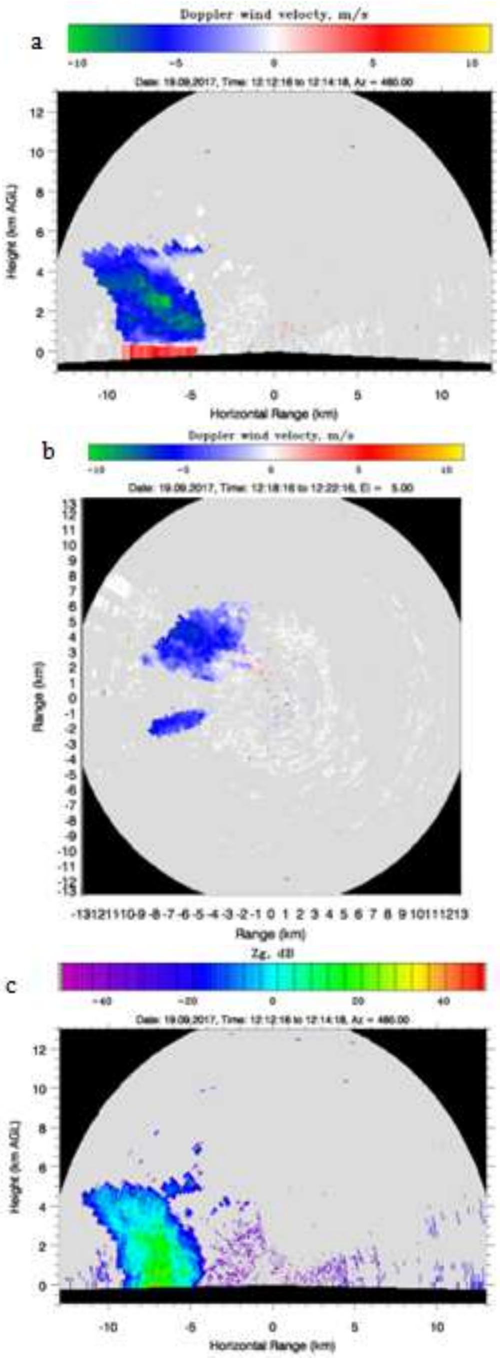

International Journal of Science and Research (IJSR)
ISSN: 2319-7064
Index Copernicus Value (2016): 79.57 | Impact Factor (2017): 7.296

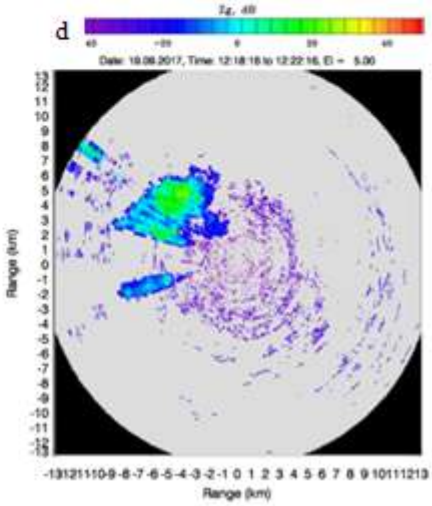


**Figure 1:** Doppler wind velocity fields observed with the MIRA-35 Doppler cloud taken in the UAE on 19.09.2017 (a) during RHI scan at 12:12 UTC, azimuth $120^0$ with wind shear, (b) during VAD scans at 12:18 UTC, $5^0$ elevation and, Observed reflectivity with the MIRA-35 Doppler cloud radar taken in the UAE on 19.09.2017 (a) during RHI scan at 12:12 UTC, azimuth $120^0$ with high RR and (c) during VAD scan at 12:18 UTC, elevation $5^0$ with high RR

### 4.2 Winter period on 16.11.2017

Formation of cloud starts 9:30 UTC when the radial wind speed is low and DWV field is S. At 9:36 UTC, the wind shear is evident as the wind speed becomes high and wind direction changes from NE below 500m to SW above 500m (figure 4-16a). With time, convergence becomes amplified leading to more cloud formation. The RHI plots show clear convergence at times 10:30, 12:15 and 12:30 UTC prior to the beginning of the precipitation (figures 2a & b). The convergence lines are mostly trending NE-SW. At 12:18 UTC, veering; clockwise change of Doppler wind field with height is also observed (figure 2b). The wind field is SE at lower height but veers to SW at higher height.

The interaction of orography, atmospheric instability, advection of warm moist air, low level wind shear and atmospheric convergence causing deep convection could have greatly amplify cloud formation processes giving rise to cumulonimbus cloud [2]. However, to determine the time of precipitation, vertical profiles are extracted from all RHI scans made on Al-Farfar mountain in the UAE on 16.11.2017 between 00:01 UTC and 23:46 UTC for each of the RR and DWV at azimuth 5100. Each of the extracted vertical profiles is then plotted as time series as shown in figure 3a & b. The time zone showing high reflectivity on the RR vertical profile which could probably due to rain are compared to its corresponding time zones on the DWV vertical profile.

The RR vertical profile shows very high reflectivity due to rain between 12:30 and 13:30 UTC. This indicates that precipitation occurs between these time. Also, the extracted RR vertical profile shows a maximum RR of 35 dB while the extracted DWV vertical profile shows a maximum DWV of 10 m/s. The observed high reflectivity before precipitation depicts thunderstorms (figure 3a &b). The life cycle of the thunderstorms starts at 10:18 UTC, when cumulus cloud is formed. At, 12:18 UTC, the thunderstorms becomes mature. By 12:48 UTC, the updraft becomes too weak to balance the downdraft, precipitation starts, leading to the dissipation of the thunderstorm.

The downward movement and very high reflectivity observed are due to the falling rain particles moving towards the earth surface after the aggregation and melting of smaller hydrometeor crystals and droplets to form larger droplets [12,13,14]. Later on, around 13:30 UTC, the cloud dissipates and rain finally stops.

Simultaneously, the precipitation data is used to verify the radar shown precipitation by plotting the hourly precipitation against the time (figure 4a). This also reiterates that precipitation takes place within the radar shown time. Furthermore, the ".BSC" files from the time series are converted to "ASCII files" so that the reflectivity and Doppler velocities values of data points could be plotted against each other (figure 4b). Although many outliers exist, the radar reflectivity and the negative Doppler wind velocity show an increasing trend with much concentration of values around radar reflectivity value of about -40 dB and Doppler wind velocity value of about -1 m/s. Finally, the EUMESAT 8 images verifies the presence of cloud over the UAE region.

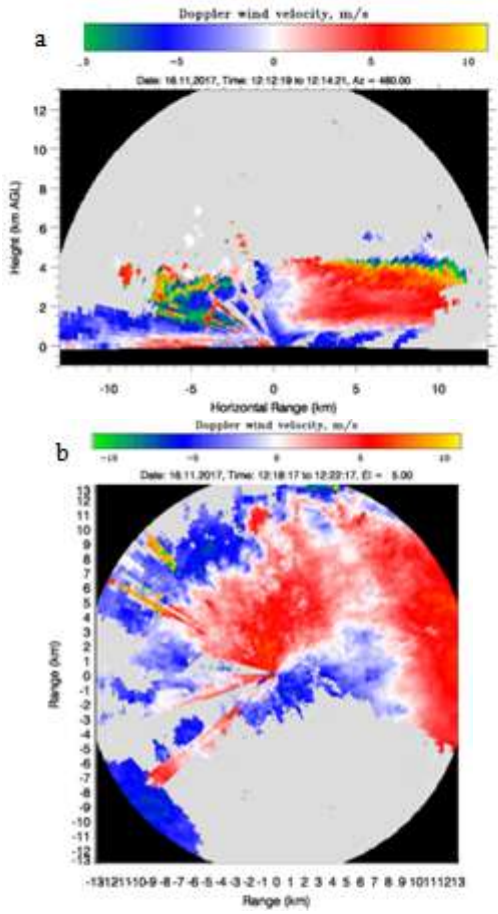

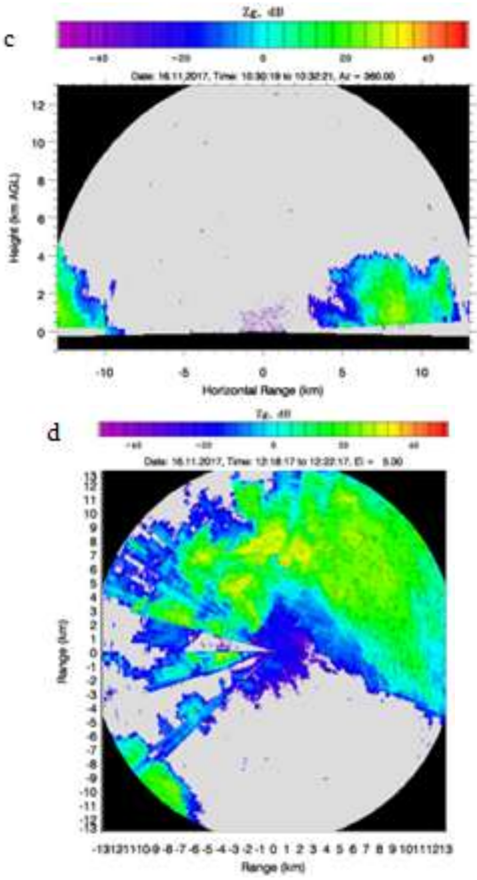


**Figure 2:** Doppler wind velocity fields observed with the MIRA-35 Doppler cloud radar scans taken in the UAE on 16.11.2017 (a) during RHI, at 12:12 UTC, azimuth $120^0$ with low level convergence and high wind shear before precipitation (b) duringVAD scans ) 12:18 UTC with SE DWV at lower height and a $90^0$ veering to SW before precipitation and, Observed reflectivity with the MIRA-35 Doppler cloud radar taken in the UAE on 16.11.2017 (c) during RHI scan at 10:30 UTC, azimuth $0^0$ with very high RR and (d) during VAD scan at 12:18 UTC, elevation $5^0$ with very high RR revealing thunderstorm at mature stage

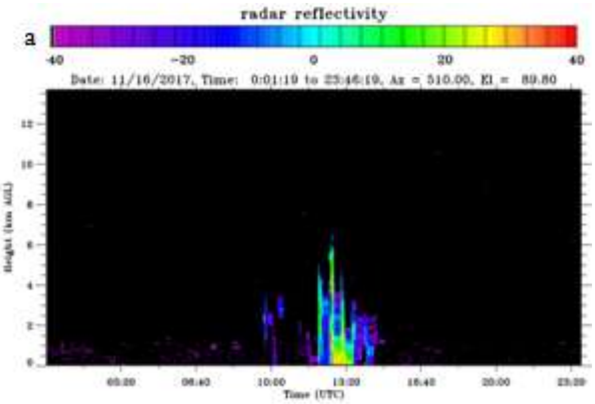


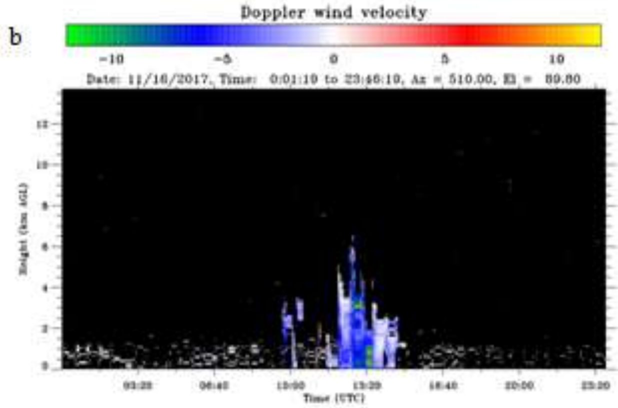


**Figure 3:** Vertical profiles extracted from all RHI scans in the UAE between 00:01 UTC and 23:46 UTC on 16.11.2017 for (a) radar reflectivity with maximum value of 35 dB and (b) Doppler wind velocity at azimuths $510^0$ with maximum value of 10 m/s.

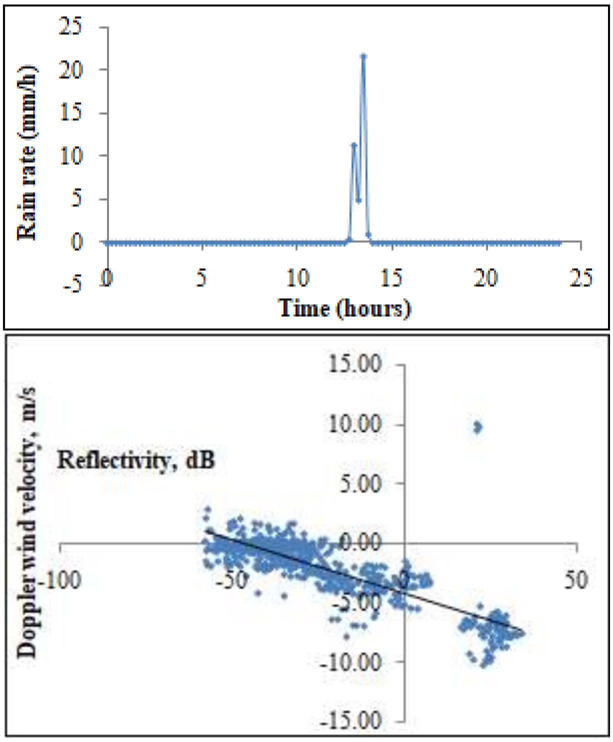


Figure 4(a) Rain rate measurements of the raingauge over Al-Farfar mountain in the UAE on 16.11.2017. There is one measurement each 15 minutes interval and (b) Doppler wind velocity against radar reflectivity data (blue dots) of the Doppler cloud radar for heights beween 288 m (range bins 1 to 10) from the vertical profiles extracted from the RHI scans (see 4-19 a & b) made on 16.11.2017. The black line is the linear regression of all data points. Although many outliers exist, the reflectivity and the negative Doppler velocity shows an increasing trend with much concentration of values around reflectivity value of about -40 dB and Doppler wind velocity value of about -1 m/s.

### 4.3 Winter period on 18.12.2017

Cloud formation begins 7:18 UTC and grows bigger. However, the clouds are so small to know the wind direction. At 7:33 UTC, the wind blows NE below 700m while it blows SW above (table 4-6). Prior to the beginning

ISSN: 2319-7064
Index Copernicus Value (2016): 79.57 | Impact Factor (2017): 7.296

of the precipitation, VAD plot at 7:48 UTC, elevation $5^0$ reveals low level convergence at the SW of the display but a low radial wind speed (figure 5a). With time, convergence becomes amplified leading to more clouds formation. The RHI plots show clear convergence at times 8:30, 9:00, 10:33 and 12:18 UTC. This is also corroborated by the VDA plots (Figures 5a & b).

The convergence lines are mostly trending NW-SE. Moreover, backing; anticlockwise wind shear with height is spotted with its characteristic backward S – shape (figure 5b). The wind direction near the radar (ground of display) is SE, backs to NE and then NW with increase in height. The interaction of orography, atmospheric instability, advection of warm moist air, low level wind shear and atmospheric convergence causing deep convection have greatly amplified cloud formation processes giving rise to cumulonimbus cloud [2]

However, to determine the time of precipitation, vertical profiles are extracted from all RHI scans made on Al-Farfar mountain in the UAE on 18.12.2017 between 12:45 and 13:30 for each of the RR and DWV at azimuth $510^0$. Each of the extracted vertical profiles is then plotted as time series as shown in figures 6a & b respectively. The time zones showing high reflectivity on the RR vertical profile which could probably due to rain are compared to its corresponding time zones on the DWV vertical profile.

The RR vertical profile shows very high reflectivity due to rain between 12:45 and 13:30. This indicates that precipitation occurs between these time. Also, the extracted RR vertcal profile shows a maximum RR of 35 dB while the extracted DWV vertcal profile shows a maximum DWV of 8.5 m/s. The observed high reflectivity before precipitation depicts thunderstorms (figure 5a & b). The life cycle of the thunderstorms starts at 07:48 UTC, when cummulus cloud is formed. At, 12:18 UTC, the thunderstorm become mature. By 12:45 UTC, the updraft becomes too weak to balance the downdraft, precipitation starts, leading to the dissipation of the thunderstorm.

Simultaneously, the precipitation data is used to verify the radar shown precipitation by ploting the hourly precipitation against time (figure 7a). This also confirms that precipitation takes place within the radar shown time. Additionally, the ".BSC files" generated from the time series plots are converted to an "ASCII file" so that the reflectivity and Doppler wind velocities values of data points could be plotted against each other (figure 7b). Although many outliers exist, the radar reflectivity and the negative Doppler wind velocity shows an increasing trend with much concentration of values around reflectivity values of -10dB and Doppler wind velocity value of -2m/s. Finally, the EUMESAT 8 images verifies the presence of cloud over the UAE region on this day.

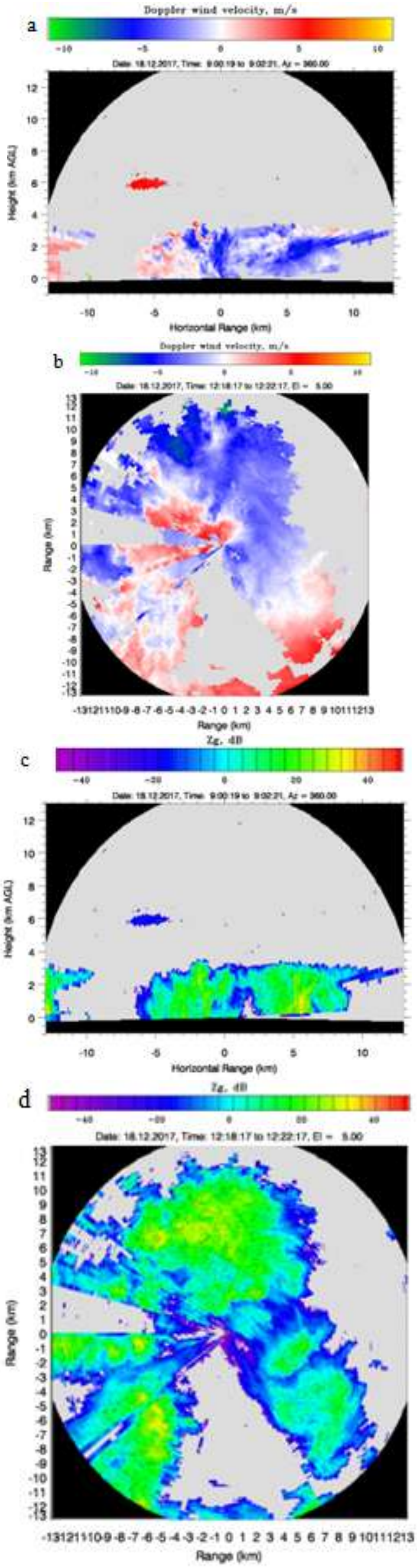


**Figure 5:** Doppler wind velocity fields observed with the MIRA-35 Doppler cloud radar taken in the UAE on 18.12.2017 (a) during RHI scans with convergence before precipitation at 09:00 UTC, $0^0$ azimuth with low level

convergence, (b) during VAD scans taken in the UAE on 18.12.2017, at 12:18 UTC, elevations $5^0$ with convergence before precipitation and high wind shear (SE DWV at low level backing to N at higher level), and Observed very high reflectivity with the MIRA-35 Doppler cloud radar taken in the UAE on 18.12.2017 before precipitation (c) during RHI scan at 09:00 UTC, azimuths $0^0$ with very high reflectivity, (d) during VAD scan at 12:18 UTC , elevation angle $5^0$ showing mature stage of a thunderstorm.

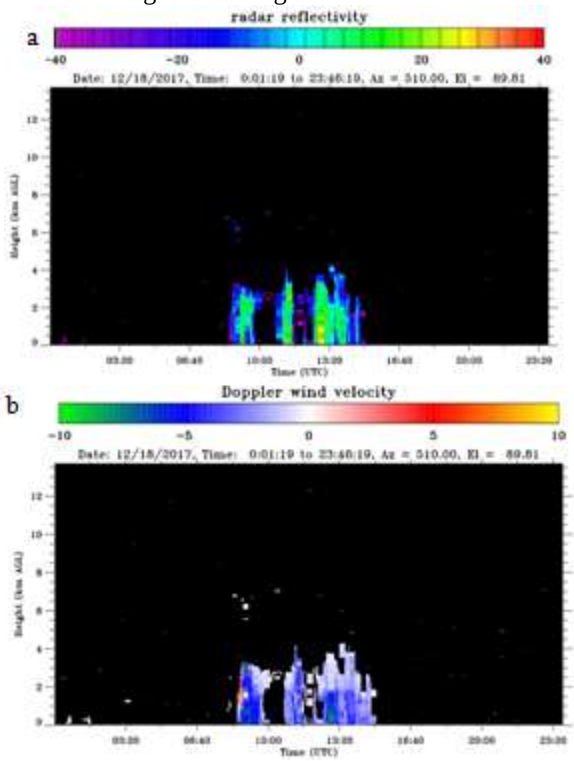


**Figure 6:** Vertical profiles extracted from all RHI in the UAE Stuttgart between 00:01 UTC and 23:46 UTC on for (a) radar reflectivity and (b) Doppler wind velocity at azimuth $510^0$. Maximum RR and DWV are up to 35 dB and 8.5 m/s respestively.

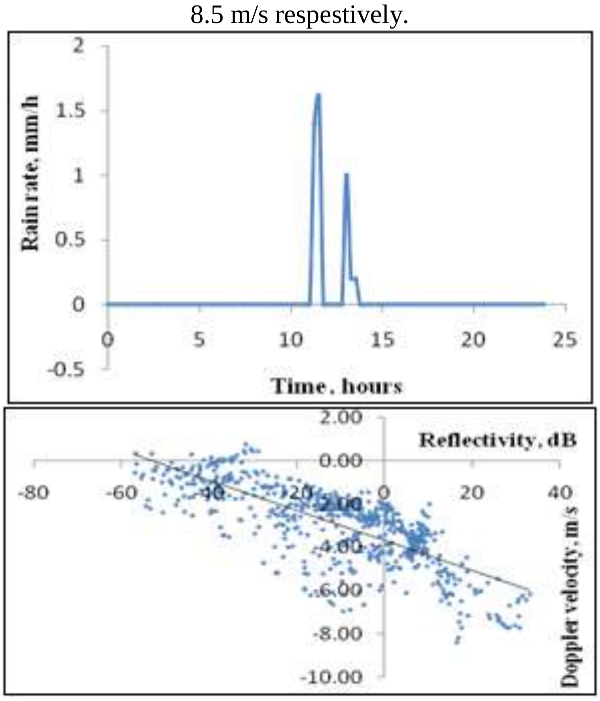


**Figure 7:** (a) Rain rate measurements of the raingauge over Al-Farfar mountain in the UAE on 18.12.2017. There is one measurement each 15 minutes interval and (b) Doppler wind velocity against radar reflectivity data (blue dots) of the Doppler cloud radar for heights beween 288 m (range bins 1 to 10) from the vertical profiles extracted from the RHI scans (see 3-17 a & b) of 18.12.2017. The black line is the linear regression of all data points. Although many outliers exist, the radar reflectivity and the negative Doppler velocity show an increasing trend with much concentration of values around reflectivity value of about -10 dB and Doppler wind velocity value of about -2 m/s.

## 5. Conclusion

In the UAE, a cumulonimbus cloud due to deep or local heating and causing convective precipitation is noticed. The wind shear including the change in wind speeds, direction and turbulent motion as well as very high reflectivity inside the cloud due to larger rain cells associated with thunderstorm are observed. On 19.09.2017, even though there is cloud formation, no precipitation occurs in the area because of very low moisture content of the advecting air during summer to sustain the cloud (forming thunderstorm). On 16.11.2017, convergence before precipitation and veering are clearly observed.

On 18.12.2017, an explicit convergence, SW of the radar display was spotted before precipitation. Mostly, the convergence lines trends SE-NW. Also, backing of wind field is obvious. Although measurement still continues in the UAE, these detected convergence zone and line provide basic insight into the ongoing OCAL project.

## 6. Future Scope

It is recommended that the scanning period of the radar be reduced so as to capture some convergence zones that start and finish quickly ahead of the radar scan period especially in the summer. Since the campaign started later than planned and less measurements were made during the last summer, therefore, next summer campaign must be looked forward to. Also, longer observations are required throughout the seasons to determine the convection initiation processes in the studied region.

## References

[1] Wulfmeyer et al. 2015
[2] Wulfmeyer et al. 2011
[3] Wulfmeyer et al. 2008
[4] Roberts and Rutledge 2003
[5] Browning et al. 1967
[6] Delanoë et al 2006
[7] Dixon and Wiener 1993
[8] Dufournet and Russchenberg 2011
[9] DWRS 2005
[10] Emanuel1994
[11] Fovell 2005
[12] Houze 1997
[13] Houze 1993
[14] Houze et al. 1989
[15] Maddox 1980
[16] Mandoos et al. 2003
[17] Mather 1991

[18] Miller 2003
[19] Orville 1996
[20] Parzen 1962
[21] Reuder and Egger 2016
[22] Rokicki and Young 1978
[23] Rosenfeld and Woodley 1993
[24] Simpson et al. 1967
[25] Steiner and Houze 1997
[26] Trentmann e al. 2009
[27] Weckwerth, 2000
[28] Willis and Heymsfield 1989
[29] Woodley 1970
[30] Al-Maskari and Gadian 2001
[31] Breed et al 2005
[32] Young 1996
[33] Yuan 2013
[34] Zong et al. 2013

## Author Profile

**Nurudeen Adesina** had bachelor degree in Geology from Obafemi Awolowo University and master degreein Earth System Science from University of Hohenheim, Germany, keen on sustainable Earth as a whole.

**List of Abbreviations**

| | |
|---|---|
| CI | Convection Initiation |
| COPS | Convection and Orographically-induced Precipitation Studies |
| DWRS | Department of Water Resources Studies |
| DWV | Doppler Wind Velocity |
| EMR | Electromagnetic Radiation |
| EUMETSAT | European Organization for the Exploitation of Meteorological Satellites KDE Kernel Density Estimation MCS Mesoscale Convective System |
| GRIB | GRIdded Binary or General Regularly-distributed Information in Binary form |
| HDF | Hierarchical Data Format |
| HDF-EOS2 | Hierarchical Data Format - Earth Observing System |
| IOP | Intensive Observation Period |
| MCS | Mesoscale Convective System |
| MSG | Meteosat Second Generation |
| NCAR | National Center for Atmospheric Research |
| NCL | NCAR Command Language |
| NetCDF | Network Common Data Form |
| OCAL | Optimization of Cloud Seeding by Advanced Remote Sensing and Land Cover Modification |
| REC | Radar Echo Classifier |
| RHI | Range Height Indicator |
| RR | Radar Reflectivity |
| RSA | Republic of South Africa |
| SEVIRI | the Spinning Enhanced Visible and InfraRed Imager |
| UAE | United Arab Emirates |
| UTC | Coordinated Universal Time |
| VAD | Velocity Azimuth Display |
| VERA | Vienna Enhanced Resolution Analysis |